

Two Simple W' Models for the Early LHC

Martin Schmaltz and Christian Spethmann

Physics Department, Boston University, Boston MA 02215

`schmaltz@bu.edu, cspeth@bu.edu`

Abstract

W' gauge bosons are good candidates for early LHC discovery. We define two reference models, one containing a W'_R and one containing a W'_L , which may serve as “simplified models” for presenting experimental results of W' searches at the LHC. We present the Tevatron bounds on each model and compute the constraints from precision electroweak observables. We find that indirect low-energy constraints on the W'_L are quite strong. However, for a W'_R coupling to right-handed fermions there exists a sizeable region in parameter space beyond the bounds from the Tevatron and low-energy precision measurements where even 50 pb^{-1} of integrated LHC luminosity are sufficient to discover the W'_R . The most promising final states are two leptons and two jets, or one lepton recoiling against a “neutrino jet”. A neutrino jet is a collimated object consisting of a hard lepton and two jets arising from the decay of a highly boosted massive neutrino.

1 Introduction

W' gauge bosons are attractive candidates for early LHC discovery. A W' with a TeV scale mass can easily be produced as an s-channel resonance from quark anti-quark initial states at the LHC. Generically, W' bosons have significant branching fractions to leptons leading to an easily observable final state. To understand the phenomenology of W' bosons it is useful to distinguish two cases: left-handed W'_L bosons couple to left-handed quarks and leptons whereas right-handed W'_R bosons couple to the right-handed fermions.

The goal of our paper is to define two simple W' models as representatives for each type and to give a broad-brush overview of their phenomenology. The models are sufficiently simple that much of the phenomenology only depends on two parameters: the mass of the W' and its universal coupling to quarks and leptons $g_{W'}$. This simplicity coupled with the possibility to vary both masses and couplings allows the models to serve as “simplified models” for LHC W' searches in the spirit of [1]. The idea is that bounds on similar models [2–15] can be obtained with relative ease by theorists by converting the bounds on the corresponding simplified models as determined by the experiments.

The simple models presented here are also sufficiently attractive to be taken seriously as specific new physics models. We determine the indirect constraints [16–18] from precision electroweak measurements and LEP2 on $M_{W'} - g_{W'}$ parameter space of each model and compare them to the direct bounds from the Tevatron [19–21] and the direct LHC reach [22–25].¹ The left panel in Figure 1 shows that the indirect constraints on W'_L models are much stronger than the Tevatron bounds for intermediate and large values of the gauge coupling $g_{W'} \gtrsim 0.5$. For example, for $g_{W'_L}$ equal to the Standard Model $SU(2)$ coupling the LHC requires an integrated luminosity of order 10 fb^{-1} to probe beyond the indirect bounds. For smaller couplings, $g_{W'} \lesssim 0.45$, about 1 fb^{-1} of data is sufficient to discover a W'_L with a mass up to 1.7 TeV. In contrast, W'_R bosons with couplings $g_{W'} \simeq 0.5$ are only loosely constrained by precision measurements and may be as light as the Tevatron bound $\gtrsim 1 \text{ TeV}$. As a result, the early LHC will probe well beyond existing bounds. For example, a W'_R with mass just beyond the Tevatron limit can already be discovered with the 2010 LHC data set corresponding to $\approx 50 \text{ pb}^{-1}$ of integrated luminosity per experiment, and would therefore be a “supermodel” in the sense of [28].

The W'_L model is based on the extended electroweak gauge group $SU(2)_1 \times SU(2)_2 \times U(1)_Y$ breaking to $SU(2)_L \times U(1)_Y$ at the TeV scale. The Standard Model fermions and Higgs transform under $SU(2)_1$ at high energies. W'_L is a linear combination of the two charged gauge bosons in $SU(2)_1 \times SU(2)_2$, it couples to all left-handed fermions and the Higgs doublet with equal strength. The constraints from low energy measurements on the W'_L mass are quite strong because amplitudes mediated by the W'_L interfere with amplitudes mediated by the Standard Model W . Such interference effects are only suppressed by $(M_W/M_{W'})^2$ and give the bounds shown in the left panel of Figure 1. At hadron colliders one searches for the W'_L with the signature of a high p_T lepton and missing energy from the decay $W'_L \rightarrow l\bar{\nu}$. The Tevatron can only compete with precision bounds at very small couplings $g_{W'} \lesssim 0.2$ whereas the LHC with 1 fb^{-1} surpasses precision bounds also for more strongly coupled W'_L bosons up to $g_{W'} \lesssim 0.45$.

The W'_R model is based on the extended electroweak gauge group $SU(2)_L \times SU(2)_R \times U(1)_{B-L}$ broken to $SU(2)_L \times U(1)_Y$ at the TeV scale. The W'_R boson couples only to right-handed quarks and leptons and does not interfere with the Standard Model W . As a result, the W'_R contributions to low-energy measurements are suppressed by $(M_W/M_{W'})^4$ and give much weaker constraints. Constraints from the Z'_R which accompanies the W'_R are still significant. We see in the right panel of Figure 1 that precision measurements allow W'_R masses as small as 500 GeV for $g_{W'} \simeq 0.5$. The lower bound on the mass depends on the Z'_R couplings which in turn depend on the embedding of the Standard Model Higgs boson in the model. This embedding introduces an additional parameter which has been projected out in Figure 1.

At hadron colliders, W'_R resonances can be discovered in hadronic final states from $W'_R \rightarrow jj$, $W'_R \rightarrow t\bar{b}$ or in leptonic channels via $W'_R \rightarrow l\bar{N} \rightarrow l\bar{l}jj$. The hadronic channels are generally more difficult but become important when the leptonic channel is closed by phase space because the right-handed neutrino N is heavier than the W'_R . Assuming that the leptonic channel is open there are two important kinematic regimes. The right-handed neutrino N may be very heavy with a mass of several 100 GeV so that all final state objects are

¹For a classic paper on W' phenomenology see [26], more recent analyses for the LHC are [27].

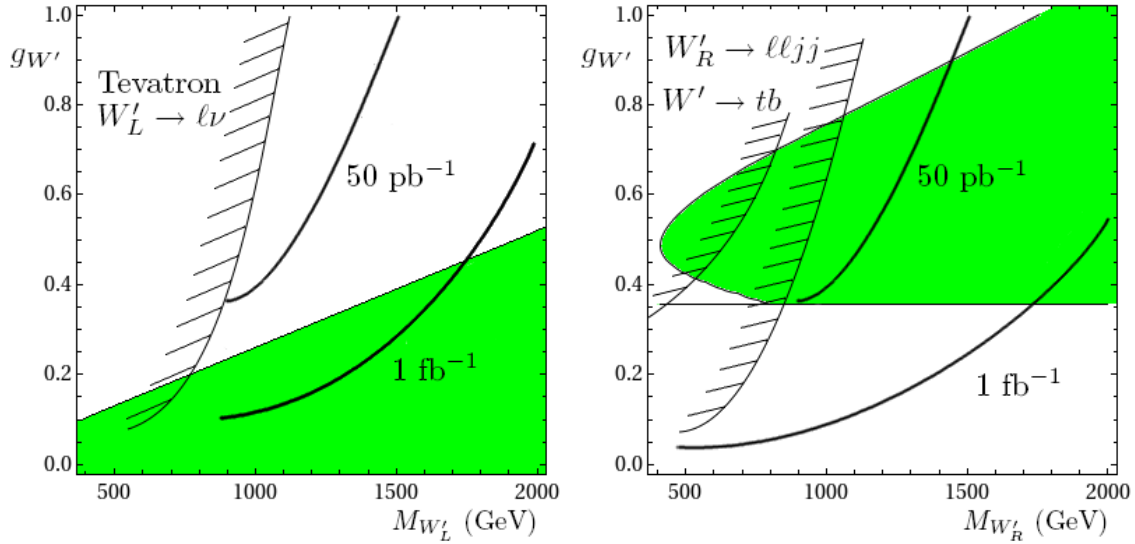


Figure 1: Experimental constraints and LHC reach for the left-handed (left) and right-handed (right) W prime as functions of the simplified model parameters $M_{W'}$ and $g_{W'}$. The plots show limits from direct searches at the Tevatron (hashed contours), the region favored by electroweak precision fits at 95 % C.L. (green/gray region), and the LHC reach at $\sqrt{s} = 7$ TeV for 50 pb^{-1} and 1 fb^{-1} of integrated luminosity.

highly energetic and well separated. In this case one would look for the final state $\bar{l}lj$ (or the lepton number violating $lljj$ final state if the right-handed neutrino has a Majorana mass). Alternatively, the right-handed neutrino might be as light as the lower bound on its mass from the non-observation of heavy neutrinos in Z decays, $M_N \gtrsim 45$ GeV. In this case the right-handed neutrino and its decay products are boosted and merge into a single massive “neutrino jet” (j_N). This is a new object consisting of two collimated subjets and an embedded hard lepton. Relatively light right-handed neutrinos with masses in the range 45 - 200 GeV thus require a search for final states with a very energetic charged lepton recoiling against the neutrino jet. Here the muonic channel is probably the most promising because it is easy to identify the embedded hard lepton inside the neutrino jet.

In Section 2 of this paper we define the two “simplified models” with W'_L and W'_R gauge bosons. Section 3 is dedicated to the calculation of contributions to precision electroweak observables and plots of the allowed parameter spaces after fitting to precision data. For the case of the W'_R the precision fit depends on the embedding of the Standard Model Higgs into the model and we discuss the different possibilities in some detail. Readers who are mainly interested in our models as simplified models are invited to skip the Section on precision electroweak constraints because such constraints can be avoided with sufficient model building ingenuity. In Section 4 we show the existing Tevatron bounds. Published W' bounds from the Tevatron refer to specific W' models with fixed values of the coupling constant $g_{W'}$. We “reprocess” the searches to extend their validity to our more general simplified models. In Section 5 we present LHC cross sections as a function of $M_{W'}$ and $g_{W'}$ for different interesting final states. Particularly promising are the $\bar{l}lj$ and lj_N signatures from decays of W'_R to heavy and light right-handed neutrinos, respectively.

The Appendices are dedicated to model building issues. In the first Appendix we consider alternate representations for the Higgses which break $SU(2)_R$. Using larger $SU(2)$ representations it is possible to raise the Z'_R mass relative to the W'_R mass. This alleviates the precision electroweak bounds from Z'_R exchange and allows even lighter W'_R bosons at the expense of slightly more complicated Higgs sectors. In the second Appendix we outline different scenarios for fermion mass generation, paying special attention to naturalness of neutrino masses.

2 Description of W' Models

2.1 The minimal W'_L Model

We start our discussion by defining a simplified model that implements a W'_L . The electroweak gauge group is extended to

$$SU(2)_1 \times SU(2)_2 \times U(1)_Y.$$

All Standard Model fermion doublets and the Higgs doublet transform under $SU(2)_1$. A bifundamental Higgs field with VEV

$$\langle \Delta \rangle = \frac{1}{\sqrt{2}} \begin{pmatrix} f & 0 \\ 0 & f \end{pmatrix}, \quad (1)$$

breaks the two $SU(2)$ factors to the diagonal $SU(2)_L$. Before electroweak symmetry breaking, the heavy gauge boson eigenstates are degenerate with mass

$$M_{Z'_L}^2 = M_{W'_L}^2 = \frac{1}{4} f^2 (g_1^2 + g_2^2). \quad (2)$$

The mixing matrix between the heavy W'_L and the Standard Model W is

$$\begin{pmatrix} W \\ W'_L \end{pmatrix} = \begin{pmatrix} \cos \theta_L & -\sin \theta_L \\ \sin \theta_L & \cos \theta_L \end{pmatrix} \begin{pmatrix} W_1 \\ W_2 \end{pmatrix}, \quad (3)$$

where

$$\sin \theta_L = \frac{g_1}{\sqrt{g_1^2 + g_2^2}}, \quad \cos \theta_L = \frac{g_2}{\sqrt{g_1^2 + g_2^2}}. \quad (4)$$

The Standard Model $SU(2)$ gauge coupling is the combination

$$\frac{1}{g^2} = \frac{1}{g_1^2} + \frac{1}{g_2^2}, \quad (5)$$

which implies $g_1, g_2 \geq g$. The heavy gauge bosons couple to the Standard Model doublets with universal coupling strength

$$g_{W'} = g \tan \theta_L. \quad (6)$$

In the special case $g_1 = g_2$ the W'_L is therefore a sequential W' , with coupling strength equal to the Standard Model gauge coupling g . Below the W'_L and Z'_L mass scale, the fermion and scalar field content of the minimal W'_L model is identical to the Standard Model.

2.2 The minimal W'_R Model

The simplest extension of the SM with a right-handed W'_R has the extended electroweak gauge group

$$SU(2)_L \times SU(2)_R \times U(1)_X,$$

with fermion charges under $U(1)_X$ equal to $(B - L)/2$. To keep our analysis general, we do not assume left-right symmetry, thus the couplings g_L and g_R are independent. Hypercharge is the combination

$$Y = T_R^3 + X \quad (7)$$

with coupling strength

$$\frac{1}{g'^2} = \frac{1}{g_R^2} + \frac{1}{g_X^2}. \quad (8)$$

Table 1: Fermion representations in the minimal W'_R model. Q^c and L^c are left-handed spinors that transform as $\mathbf{2}$'s under $SU(2)_R$. N is a gauge singlet fermion which was included to allow a Dirac mass with the right-handed neutrino ν^c .

	X	T_R^3	Y
Q	1/6	0	1/6
$Q^c = \begin{pmatrix} u^c \\ d^c \end{pmatrix}$	-1/6	$\mp 1/2$	$\begin{pmatrix} -2/3 \\ 1/3 \end{pmatrix}$
L	-1/2	0	-1/2
$L^c = \begin{pmatrix} \nu^c \\ e^c \end{pmatrix}$	1/2	$\mp 1/2$	$\begin{pmatrix} 0 \\ +1 \end{pmatrix}$
N	0	0	0

In particular, this equation implies $g_X, g_R > g'$. We assume the minimally required scalar sector at the $SU(2)_R$ breaking scale, which consists of a single $SU(2)_R$ doublet. This scalar doublet carries a $U(1)_X$ charge of $+1/2$, so that one of the components has zero hypercharge. The scalar acquires a VEV

$$\langle H_R \rangle = \frac{1}{\sqrt{2}} \begin{pmatrix} 0 \\ f \end{pmatrix} \quad (9)$$

which breaks $SU(2)_R \times U(1)_X$ down to $U(1)_Y$. Neglecting electroweak symmetry breaking, the heavy gauge boson masses are

$$M_{W'_R}^2 = \frac{1}{4} f^2 g_R^2, \quad M_{Z'_R}^2 = \frac{1}{4} f^2 (g_R^2 + g_X^2). \quad (10)$$

in complete analogy to the Standard model. The neutral gauge boson mixing matrix is

$$\begin{pmatrix} Z'_R \\ B \end{pmatrix} = \begin{pmatrix} \cos \theta_R & -\sin \theta_R \\ \sin \theta_R & \cos \theta_R \end{pmatrix} \begin{pmatrix} W_R^3 \\ X \end{pmatrix}, \quad (11)$$

where X is the $U(1)_X$ gauge boson and

$$\sin \theta_R = \frac{g_X}{\sqrt{g_X^2 + g_R^2}}, \quad \cos \theta_R = \frac{g_R}{\sqrt{g_X^2 + g_R^2}}. \quad (12)$$

The coupling strength g_R of the W'_R boson is bounded from below by the hypercharge coupling g' , whereas the W'_L coupling can be arbitrarily small. The required fermion representations in the W'_R model (including a right-handed neutrino and a gauge singlet N) are shown in Table 1.

2.3 Higgs Sector in the W'_R Model

To keep the analysis general, we include two Higgs electroweak symmetry breaking representations,

1. An $SU(2)_L \times SU(2)_R$ bidoublet ϕ with zero $U(1)$ charge, and
2. An $SU(2)_L$ left-handed doublet H_L with $U(1)$ charge $+1/2$.

After $SU(2)_R$ breaking, the bidoublet decomposes into two $SU(2)_L$ doublets with hypercharges $\pm 1/2$. The two fields ϕ and H_L acquire VEVs

$$\langle \phi \rangle = \frac{1}{\sqrt{2}} \begin{pmatrix} \kappa & 0 \\ 0 & \kappa' \end{pmatrix}, \quad \langle H_L \rangle = \frac{1}{\sqrt{2}} \begin{pmatrix} 0 \\ v_L \end{pmatrix}. \quad (13)$$

Since both $\langle\phi\rangle$ and $\langle H_L\rangle$ contribute to electroweak gauge boson masses, the VEVs have to satisfy the relation $\kappa^2 + \kappa'^2 + v_L^2 = v^2 = (246 \text{ GeV})^2$. Important special cases are $\kappa = \kappa' = 0$ or $v_L = 0$ for which the precision electroweak constraints are the same as in a model which contains only one of the electroweak symmetry breaking fields (H_L or ϕ).

Fermion masses may be generated from renormalizable Yukawa interactions with the bifundamental Higgs doublet ϕ and/or from dimension five operators with the H_L and H_R doublets,

$$\mathcal{L}_Y = \lambda_{\phi q} Q\phi Q^c + \frac{\lambda_{hq}}{\Lambda} QH_L\tilde{H}_R Q^c, \quad (14)$$

plus possibly couplings of these fields with epsilon contractions of $SU(2)_L$ indices. Additional Yukawa interactions may be present to generate first and second generation quark masses, as well as lepton masses. However, the fit to precision data as well as the W'_R phenomenology is independent of quark and charged lepton masses. Right-handed neutrinos have to be massive and decay promptly to a lepton plus two jets. Their masses can be Dirac or Majorana, affecting the W'_R decay signature, but not the precision fit. For completeness, we briefly discuss fermion masses in the Appendix.

3 Electroweak Precision Constraints

3.1 Constraints on the W_L model

Following Han and Skiba [30], we quantify the impact of new physics on electroweak precision observables by calculating the coefficients of 21 dimension six operators of Standard Model fermions and the Higgs field. In the W'_L and W'_R models the constrained operators are induced by the exchange of scalars and of the heavy gauge bosons W' and Z' .

Let us turn our attention to scalar exchange first. Because of Lorentz invariance, scalar fields can couple to fermion bilinears, but not to covariant derivatives of the Standard Model Higgs. Therefore scalar exchange can only generate the four-fermion operators considered by Han and Skiba. Of those, only the ones involving first generation quarks and leptons are strongly restricted by electroweak precision measurements. In our models, the contribution of scalar exchange to such operators is small because the Yukawa coupling coefficients are proportional to the fermion masses. We will therefore concern ourselves only with contributions due to heavy gauge boson exchange.

In the W_L model before electroweak symmetry breaking, the three heavy gauge bosons $W'_L{}^\pm$ and Z'_L transform as a triplet under $SU(2)_L$. They couple to the current

$$J_{W'_L}^{\mu,a} = g_{W'} [\ell^\dagger \bar{\sigma}^\mu T^a \ell + q^\dagger \bar{\sigma}^\mu T^a q + (ih^\dagger T^a D^\mu h + \text{h.c.})], \quad (15)$$

where $T^a = \frac{1}{2}\tau^a$ are the $SU(2)_L$ group generators. The effective Lagrangian is then

$$\mathcal{L}_{\text{eff}} = \mathcal{L}_{\text{SM}} - \frac{1}{2} \frac{1}{M_{W'_L}^2} J_\mu^a J^{\mu,a}, \quad (16)$$

so that the coefficients of the triplet operators in Han and Skiba's formalism are universal

$$a_t = -\frac{1}{4} \frac{g_{W'_L}^2}{M_{W'_L}^2}. \quad (17)$$

The results of the electroweak fit of the W'_L model are shown as shaded contours in Figure 7.

3.2 Z' Currents and Charges in the W'_R model

In the W'_R model the situation is more complicated, since the W'_R and Z'_R do not transform as an irreducible representation of the Standard Model gauge group. It is therefore necessary to examine Z'_R and W'_R exchange separately. As we will see below, only the Z'_R produces strongly constrained operators. We start by calculating the couplings of the fermions and the two Higgs representations to the Z'_R .

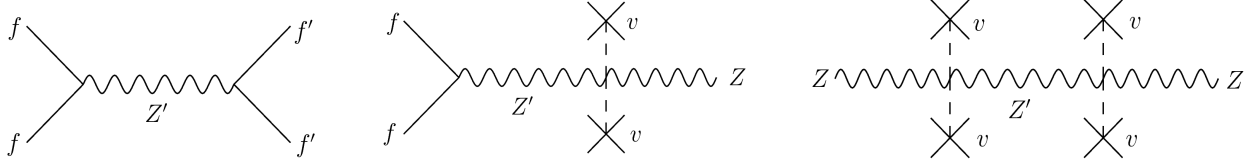


Figure 2: Dimension six operators from Z' exchange: a) Four fermion couplings, b) Corrections to the fermion-Z coupling, c) Mass shift for the Z, which contributes to the T-parameter.

The fermion contribution to the Z'_R current is

$$J_{Z'_R}^\mu(f) = \sum_f (g_R \cos \theta_R T_R^3 - g_X \sin \theta_R X) f^\dagger \bar{\sigma}^\mu f. \quad (18)$$

The operator description by Han and Skiba is formulated in terms of a single Higgs doublet, so at first glance it would appear that additional scalar representations cannot be accommodated in this formalism. However, the VEV is the only component of the Higgs field that has been measured so far and is therefore relevant for the electroweak fit. The left-handed doublet contribution to the Z'_R current is

$$J_{Z'_R}^\mu(H_L) = -i \frac{1}{2} g_X \sin \theta_R H_L^\dagger D^\mu H_L + \text{h.c.} \xrightarrow{\text{EWSB}} -\frac{1}{4} v_L^2 (g'^2 + g_L^2)^{1/2} g_X \sin \theta_R Z^\mu. \quad (19)$$

Similarly, the contribution of the Higgs bidoublet is

$$J_{Z'_R}^\mu(\phi) = i g_R \cos \theta_R \text{tr} [(T_3^R \phi)^\dagger (D^\mu \phi)] + \text{h.c.} \xrightarrow{\text{EWSB}} \frac{1}{4} (\kappa^2 + \kappa'^2) (g'^2 + g_L^2)^{1/2} g_R \cos \theta_R Z^\mu. \quad (20)$$

We can therefore represent the scalar sector contribution to the Z'_R current in terms of a single Higgs field h with VEV v as in the Standard Model,

$$\begin{aligned} J_{Z'_R}^\mu(h) &= \frac{1}{2} \left(\frac{\kappa^2 + \kappa'^2}{v^2} g_R \cos \theta_R - \frac{v_L^2}{v^2} g_X \sin \theta_R \right) [i(h^\dagger D^\mu h) + \text{h.c.}] \\ &= \frac{1}{2} \sqrt{g_R^2 + g_X^2} \left(\cos^2 \theta_R - \frac{v_L^2}{v^2} \right) [i(h^\dagger D^\mu h) + \text{h.c.}] \end{aligned} \quad (21)$$

Z'_R exchange generates three different kinds of dimension six operators, as shown in Fig. 2. The first of those are four fermion interactions, which are represented by the operators

$$a_{ij}^{(s)} \mathcal{O}_{ij}^{(s)} = -\frac{4}{f^2} \left(\cos^2 \theta_R T_{R,i}^3 - \sin^2 \theta_R X_i \right) \left(\cos^2 \theta_R T_{R,j}^3 - \sin^2 \theta_R X_j \right) f_i^\dagger \bar{\sigma}^\mu f_i f_j^\dagger \bar{\sigma}_\mu f_j. \quad (22)$$

The operators that modify fermion-Z couplings are

$$a_{hi}^{(s)} \mathcal{O}_{hi}^{(s)} = -i \frac{2}{f^2} \left(\cos^2 \theta_R - \frac{v_L^2}{v^2} \right) \left(\cos^2 \theta_R T_{R,i}^3 - \sin^2 \theta_R X_i \right) (h^\dagger D_\mu h) f_i^\dagger \bar{\sigma}^\mu f_i + \text{h.c.} \quad (23)$$

Finally, the Z mass is shifted by the T operator

$$a_h \mathcal{O}_h = -\frac{2}{f^2} \left(\cos^2 \theta_R - \frac{v_L^2}{v^2} \right)^2 |h^\dagger D_\mu h|^2. \quad (24)$$

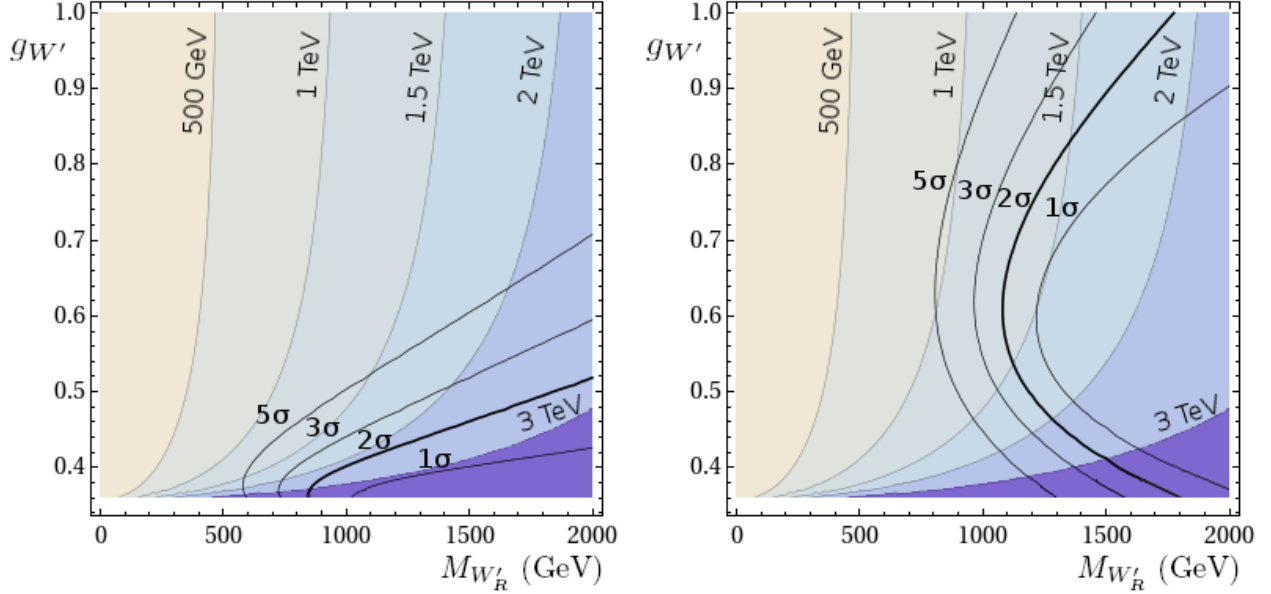


Figure 3: Contour plots of electroweak precision exclusion levels and the Z'_R mass in the W'_R model as a function of the W'_R mass and the right-handed coupling constant $g_{W'} = g_R$. Left: Purely bidoublet VEV ($v_L = 0$), Right: purely left-handed doublet VEV ($v_L = v$).

Exchange of the W'_R does not generate four fermion operators with strong constraints from electroweak precision measurements. However, one might be concerned that mixing with the Standard model W shifts the mass of the W mass eigenstate and therefore contributes to the ρ parameter. Diagonalizing the mass-squared matrix for the charged gauge bosons and expanding in powers of v^2/f^2 , we find

$$\frac{\delta M_W}{M_W} = -\frac{2\kappa\kappa'}{f^2} + \mathcal{O}(v^4/f^4). \quad (25)$$

To reproduce the large top/bottom mass hierarchy, at least one of the two bidoublet VEVs must be much smaller than the electroweak symmetry breaking scale v . Thus the W'_R mass shift contribution to the ρ parameter has an additional suppression beyond the v^2/f^2 present in the contribution to $\delta\rho$ from $Z'_R - Z$ mixing. We will therefore neglect W'_R exchange.

The dimension 6 operators generated by Z'_R exchange depend on 3 model parameters: the scale of $SU(2)_R$ breaking f , the right-handed gauge boson mixing angle $\tan\theta_R = g_X/g_R$, and the fraction of the electroweak symmetry breaking vev squared v_L^2/v^2 contained in H_L . Since we will be interested in W' phenomenology, it is convenient to change variables from f and θ_R to the more experimentally relevant $g_R = g'/\sin\theta_R$ and the W'_R mass $m_{W'_R} = g_R f/2$. For the remaining parameter, v_L^2/v^2 , we focus on three representative cases $v_L = 0, v_L = v$, and $v_L = v/\sqrt{2}$.

3.3 Bidoublet Higgs

Let us first consider the case where only the bidoublet has a VEV, $v_L = 0$. Since we can neglect scalar exchange contributions in the electroweak fit, this limit is equivalent to removing H_L completely. The result of our fit to the precision observables for this case is shown in the left plot in Fig. 3. Note that there is a minimum theoretically allowed value for the W'_R coupling $g_R = g'$. This value corresponds to the limit $g_X \rightarrow \infty$. The Figure shows that for a given $M_{W'_R}$, the smallest possible values of g_R (and very large g_X) are preferred. This is easy to understand by noticing that the strongly constrained operators \mathcal{O}_{hf} and \mathcal{O}_h

in Eq. 23 are both proportional to powers of $\cos \theta_R = g'/g_X$. In the preferred region of parameter space the Z'_R is very heavy and out of reach of the early LHC.

In the rest of this subsection we will briefly elaborate on the precision fit in the limit of large g_X and examine whether a large value for the g_X coupling constant is reasonable from a model building perspective.

In the limit of $g_X \gg g'$, the electroweak constraints are particularly easy to understand because only the four fermion operators in Eq. 23 survive. Furthermore, we have in this limit

$$a_{\mathbb{F}' } \propto \frac{g_X^2}{M_{Z'_R}^2} = \frac{4g_X^2}{(g_X^2 + g_R^2)f^2} \rightarrow \frac{4}{f^2}. \quad (26)$$

The most stringent constraint on these four-fermion operators comes from measurements of $e^+e^- \rightarrow e^+e^-$ scattering at LEP II [31] and bounds the operator

$$\mathcal{O}_{4e} = \frac{2\pi}{(\Lambda_{ee}^-)^2} \bar{e}\gamma_\mu e \bar{e}\gamma^\mu e. \quad (27)$$

This operator is precisely the one generated by exchange of the Z'_R in our model in the limit of large g_X because the Z'_R couplings become left-right symmetric. The experimental bound on Λ_{ee}^- implies a limit of $f \geq 5.1$ TeV at the 95 % confidence level. Since $g_R \approx g'$ we then obtain the minimum allowed W'_R mass as $M_{W'_R} \geq fg'/2 \approx 900$ GeV, which reproduces the lower bound on W'_R masses in our plot.

We now briefly examine what a reasonable upper bound on the allowed values for g_X might be. Large values for the gauge coupling of a $U(1)$ gauge group are a concern as they increase in the UV due to running and require new physics before they become non-perturbatively large. One possibility for this new physics is that the $U(1)$ gauge group is embedded in a non-abelian group, thereby turning around the sign of the beta function. Here, a particularly nice possibility for the embedding of $U(1)_X$ would be to consider near-TeV scale gauge “unification”

$$SU(3)_{\text{color}} \times U(1)_X \subset SU(4), \quad (28)$$

motivated by the fermion charges which naturally fit into this group. Using the $SU(4)$ normalization of $g_X = \sqrt{3/2} g_3$ and neglecting the running of the gauge couplings between the unification scale and the TeV scale, we obtain $g_X \approx 1.5$. This value of the coupling lies in the preferred region of the model parameter space.

3.4 Left-Handed Higgs

We now consider the opposite case, a Higgs VEV only for the $SU(2)_L$ doublet H_L , $v_L = v$. This is equivalent to eliminating the bidoublet Higgs field from the theory. The T -operator from Z' exchange becomes

$$a_h \mathcal{O}_h = -\frac{2}{f^2} \sin^4 \theta_R |h^\dagger D_\mu h|^2, \quad (29)$$

and the fermion-Higgs coupling operators are

$$a_{hi}^{(s)} \mathcal{O}_{hi}^{(s)} = -i \frac{2}{f^2} \sin^2 \theta_R \left(\cos^2 \theta_R T_{R,i}^3 - \sin^2 \theta_R X_j \right) (h^\dagger D_\mu h) f_i^\dagger \bar{\sigma}^\mu f_i + \text{h.c.} \quad (30)$$

Which region of parameter space is now preferred? The Higgs couplings are suppressed for small $\sin \theta_R = g'/g_R$, thus preferring small values of g_X . However, the Z' couplings to fermions in Eq. 18 prefer a value of $\tan \theta_R$ which minimizes the couplings to charged leptons because they are most strongly constrained by LEP measurements. This competition leads to a broader distribution of the preferred values of g_R . The resulting exclusion plot is shown in the right half of Fig. 3. The electroweak fit predicts a more strongly coupled W'_R , $M_{Z'}$ relatively close to $M_{W'}$, and small Z' couplings to charged leptons.

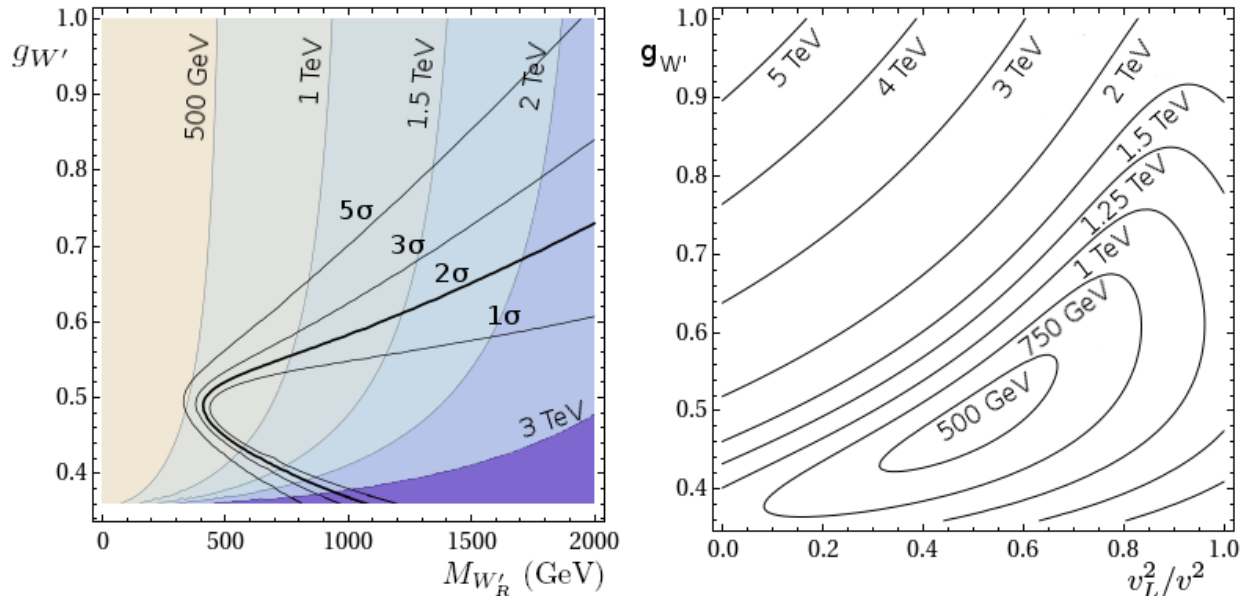


Figure 4: Left: Electroweak constraints on the Hybrid Higgs model for $(v_L/v)^2 = 1/2$. Right: Minimally allowed W' mass (in units of GeV) as a function of $(v_L/v)^2$ and g_R .

3.5 Hybrid Higgs

Finally, we discuss the general case where both electroweak breaking VEVs are non-zero. In the left half of Fig. 4 we set the Higgs VEVs for both fields ϕ and H_L to $v/\sqrt{2}$ and plot electroweak precision constraints on the parameter space of the resulting model. There is a narrow region where a W'_R with a mass ≈ 400 GeV is allowed. This region of parameter space appears fine-tuned. To investigate the degree of fine-tuning necessary to obtain such a small W'_R masses, we plot the minimal allowed W'_R mass as function of the model parameters $(v_L/v)^2$ and g_R (right half of Fig. 4).

From the figure it is evident that the precision fit prefers a narrow band in parameter space centered around $v_L \approx v_\phi \approx v/\sqrt{2}$ and $g_R \approx g_X \approx \sqrt{2}g'$. In this region, the Z' couplings to the two Higgs representations cancel, and there are consequently no constraints from the T parameter or from shifts of the Z coupling to fermions. In addition, setting the gauge coupling constants equal decouples the right-handed electron from the Z' , since for this field the X and T_R^3 charges are identical. Electroweak precision measurements therefore place weak bounds on such a Z' , allowing the scale f and the W'_R mass to be low.

In this model there is no symmetry reason for why the VEVs of scalars in different representations should be equal or why the coupling constants of the $SU(2)_R$ and $U(1)_X$ gauge groups should be equal. Thus maybe W'_R masses of order 1 TeV corresponding to more generic regions of parameter space should be considered more natural. However, it is remarkable that a Z' boson with the relatively strong couplings $g_R = g_X = \sqrt{2}g'$ is consistent with the precision data for masses as low as $m_{Z'_R} \sim 570$ GeV, allowing $M_{W'_R} \sim 400$ GeV.

As we will see in the next section, direct searches from the Tevatron imply much stronger limits on the W'_R mass. The fit to precision electroweak observables of our model with $(v_L/v)^2 = 1/2$, $g_R = g_X$ and $M_{W'_R} = 1$ TeV is better than the Standard Model fit, with $\Delta\chi^2 = -2.0$.

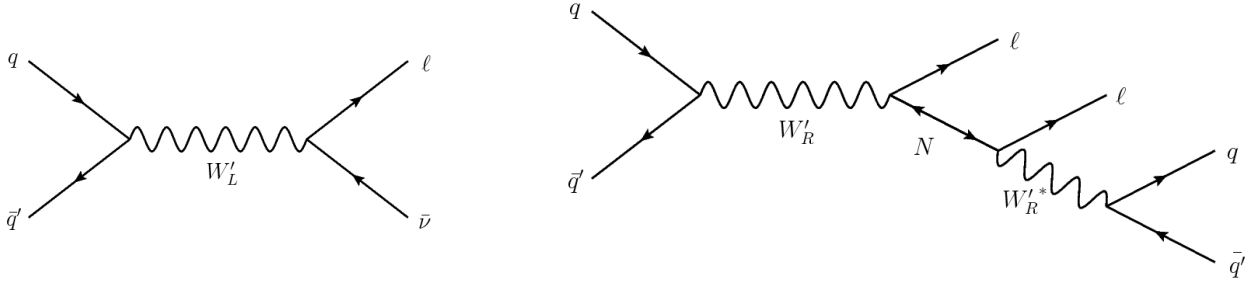


Figure 5: Left: Decay of the W'_L to a lepton and anti-neutrino. Right: Decay of the W'_R to a same sign dilepton and two jets via a right-handed Majorana neutrino and a virtual W'_R .

4 Tevatron Exclusion Limits

4.1 Tevatron Limits on $W'_L \rightarrow l\nu$

The CDF and DØ experiments at the Tevatron have searched for signatures of W' bosons decaying in both leptonic and hadronic channels. We will first compare the results from the most recent DØ search for $W'_L \rightarrow e\nu_e$ [19] with electroweak precision limits from LEP2. In the Tevatron study, a set of inclusive single electron and missing energy cuts were applied on a data sample of $\approx 1 \text{ fb}^{-1}$. After reconstruction, two events with transverse mass $m_T > 500 \text{ GeV}$ were found. Taking into account statistical and systematic backgrounds, the DØ collaboration concluded that a sequential W'_L with SM strength coupling to electrons and Standard Model neutrinos can be excluded for $M_{W'_R}$ up to 1 TeV at the 95 % C.L.

To understand which other values of W'_L masses and couplings this search was sensitive to, we used MADGRAPH [33] to simulate 1000 parton level events at each of 210 model points with W'_L masses between 500 GeV and 1500 GeV and gauge coupling constants between 0.05 and 1. Since initial state radiation is not included in MADGRAPH, the W'_L resonance is always produced without transverse momentum in the simulated events. The transverse momenta of the lepton and neutrino are then equal and opposite, and the transverse mass of the W'_L is

$$m_T(W'_L) = 2p_T(l). \quad (31)$$

Counting events with lepton $p_T > 250 \text{ GeV}$ ($m_T > 500 \text{ GeV}$) and $|\eta_e| < 1.1$, we find that with 1 fb^{-1} of integrated luminosity 3.0 events would be expected for a sequential W'_L at $M_{W'_L} = 1 \text{ TeV}$. Approximating the signal acceptance as independent of phase space, we use this number of events to find the 95 % C.L. exclusion limit for different coupling strengths and masses. The resulting Tevatron exclusion limit is shown as a hashed contour in Figure 1. In the most common models (e.g. KK gauge bosons modes, Little Higgs) a W'_L is accompanied by a Z' with equal mass and coupling strength, and LEP2 data excludes such a Z'_L with a mass up to 2.6 TeV. Our derived Tevatron bound is only competitive for coupling constants less than $g_R = 0.2$. At such small coupling, the early LHC cannot reach beyond the Tevatron bound.

4.2 Tevatron Limits on $W'_R \rightarrow eejj$

The results from the above search do not apply to the W'_R decaying to a lepton and an unstable heavy neutrino, since such events do not produce missing energy. The Tevatron collaborations have not published any search results for $W'_R \rightarrow lljj$ decays. There are however several searches for leptoquark pair production, which shares the same final $eejj$ and $\mu\mu jj$ states [34, 35]. Because of the different event topology, those results are not directly applicable to the W'_R simplified model. However, the production and decay of W'_R resonances (with subsequent decay of heavy right-handed neutrinos) would be noticeable in those data analyses as a surplus of events with large dilepton invariant mass and large scalar transverse momentum

sum. We therefore re-interpreted the Tevatron leptoquark search to extract limits on the W_R resonance mass and coupling strength.

As will be described in more detail in the LHC section, the $\mu\mu jj$ final state is more sensitive to the W'_R decay signal because of reduced lepton isolation requirements. It would therefore appear that using the DØ second generation leptoquark search would yield stronger limits on the simplified model parameter space. However, the $\mu\mu jj$ study uses a multivariate analysis to distinguish the leptoquark signal from background including cuts on μj invariant masses, which are not meaningful for right-handed neutrino decay. The first generation leptoquark search instead uses cuts on the dilepton mass and the total transverse momentum. We therefore apply our signal to the selection cuts of the first generation leptoquark search.

To estimate the maximum mass of a W'_R that would have been visible at the Tevatron, we perform a scan over W'_R masses in the range 500-1200 GeV and right-handed neutrino masses up to $M_{W'_R}$ using the left-right model included in PYTHIA 8.1 [36]. The analysis was performed at the parton level. Detector effects are approximated by smearing the energies of electrons and jets according to a Gaussian with standard deviation

$$\sigma_E = a \cdot \sqrt{E} \oplus b \cdot E, \quad (32)$$

where the Energy is measured in GeV and \oplus stands for adding in quadrature. For the constants we choose

$$a_{\text{jet}} = 0.80, \quad b_{\text{jet}} = 0.05, \quad a_e = 0.20, \quad b_e = 0.01, \quad (33)$$

following [37]. After energy smearing, we apply a set of kinematic and isolation cuts:

- For each electron-jet pair and jet-jet pair, $\Delta R > 0.5$
- For any electron and any jet, $p_T > 25$ GeV
- At least one of the two electrons must be central, $|\eta_e| < 1.1$, and both electrons must be within the electromagnetic calorimeter, $|\eta_e| < 1.1$ or $1.5 < |\eta_e| < 2.5$
- Both jets must be within the hadronic calorimeter, $|\eta_j| < 2.5$

Finally, we apply the background rejection cuts of the first generation leptoquark analysis of $m_{ee} > 110$ GeV and $\sum p_T > 400$ GeV.

In the left part of Figure 6, we plot the cross section for signal events that pass the leptoquark search cuts as a function of the W'_R and the heavy neutrino mass for the left-right symmetric case $g_L = g_R$. In the right half of the figure we show the signal acceptance.

In the Introduction (right half of Fig. 1), we show the resulting exclusion line for different values of the right-handed gauge coupling, assuming that the right-handed neutrino mass is close to the optimal value of 300 GeV. In making the introduction plot we assumed that five signal events are sufficient for the signal to be visible.

4.3 Tevatron Limits on $W'_{L/R} \rightarrow jj/tb$

Even if the decay of the right-handed W'_R to leptons is kinematically allowed, the Tevatron searches would have been unable to see the signal in the following cases:

1. If $m_N \approx M_{W'_R}$, the branching ratio to leptons becomes small, reducing the effective cross section.
2. For neutrino masses below 100 GeV, the two jets and the electron from the neutrino decay can not be sufficiently separated. The leptoquark search is therefore not sensitive to a $W_R \rightarrow eejj$ decay signal in this mass region.

To assure that a W'_R with suppressed leptonic decay modes has not been missed, it is necessary to compare the above result with the search for W' resonances in the jj and tb final states, which arise from W' decays to quarks. The CDF collaboration has searched for resonances in the dijet invariant mass spectrum, and

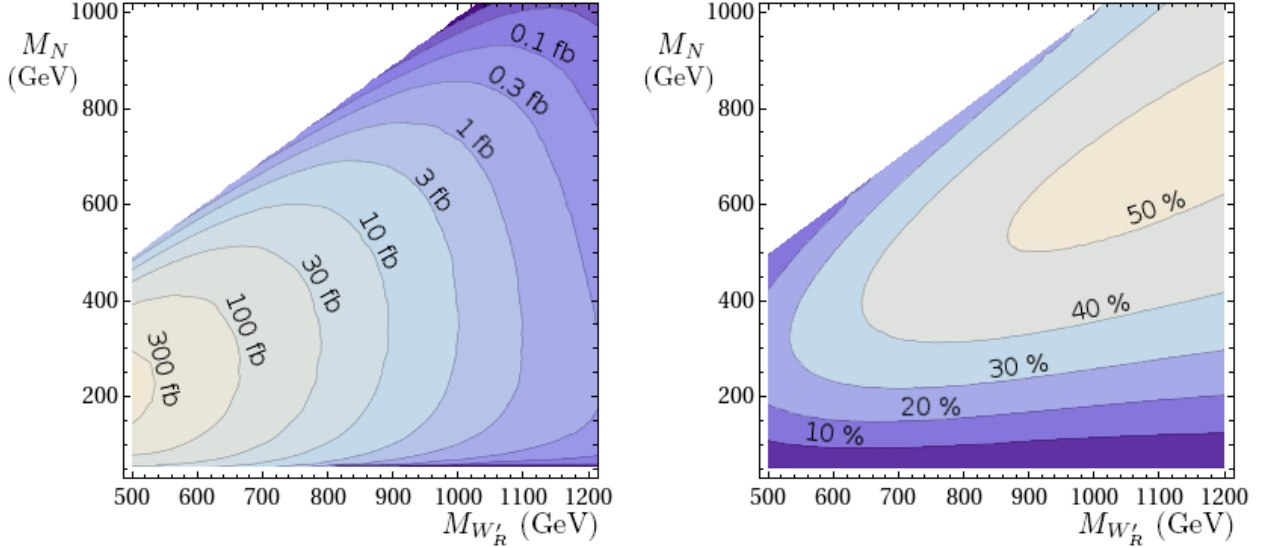


Figure 6: Left: Effective Tevatron cross section for $W'_R \rightarrow jjee$ signal events after first generation leptoquark search cuts as described in the text. The gauge coupling constant is assumed to be $g_R = g$. The LEP excluded region ($M_N < 45$ GeV) has been omitted. Right: Signal acceptance as a function of the same variables.

found that a W' with Standard Model couplings can be excluded up to $M_{W'} = 800$ GeV [20]. Since the width of the resonance depends on the coupling strength, this result cannot be extended to other values of g_R in a straightforward way. The DØ collaboration has searched for the decay of a resonance into top+bottom quarks, and found a limit of 740 GeV for a W' with SM coupling g [21]. The mass limits from this search for different values of the gauge coupling strength are included in Fig. 1.

5 LHC Reach

For the left-handed W'_L and the right-handed W'_R which we consider in this paper the W' couplings to fermions are universal. This makes the determination of branching fractions particularly simple. Neglecting fermion masses, the branching fractions of the W' are 1/12 for each generation of leptons and 1/4 for each generation of quarks. The comparatively large branching fraction to leptons of 1/6 (eN_e and μN_μ combined) makes the W' a favorable search target for the early LHC. In the following we will concentrate on the leptonic decay mode

$$W'_{R/L}{}^\pm \rightarrow l^\pm N.$$

Here N is either the Standard Model left-handed neutrino in the case of a W'_L or the heavy right-handed neutrino in the left-right model.

The ATLAS collaboration has published a detailed study of both $W'_L \rightarrow l\nu$ and $W'_R \rightarrow lN \rightarrow lljj$ events at the 14 TeV LHC [22]. For the right-handed W'_R two model points were investigated in detail, including all Standard Model backgrounds and a full detector simulation. The gauge coupling constant was assumed to be equal for the left-handed and right-handed $SU(2)$ groups.

To compare the early LHC reach with the results from our electroweak fit, it is necessary to generalize this analysis to arbitrary values of the $W'_{L/R}$ mass, right-handed neutrino mass and gauge coupling strength. We therefore again perform a parton level scan over the parameter space. The details of our analysis will be described below.

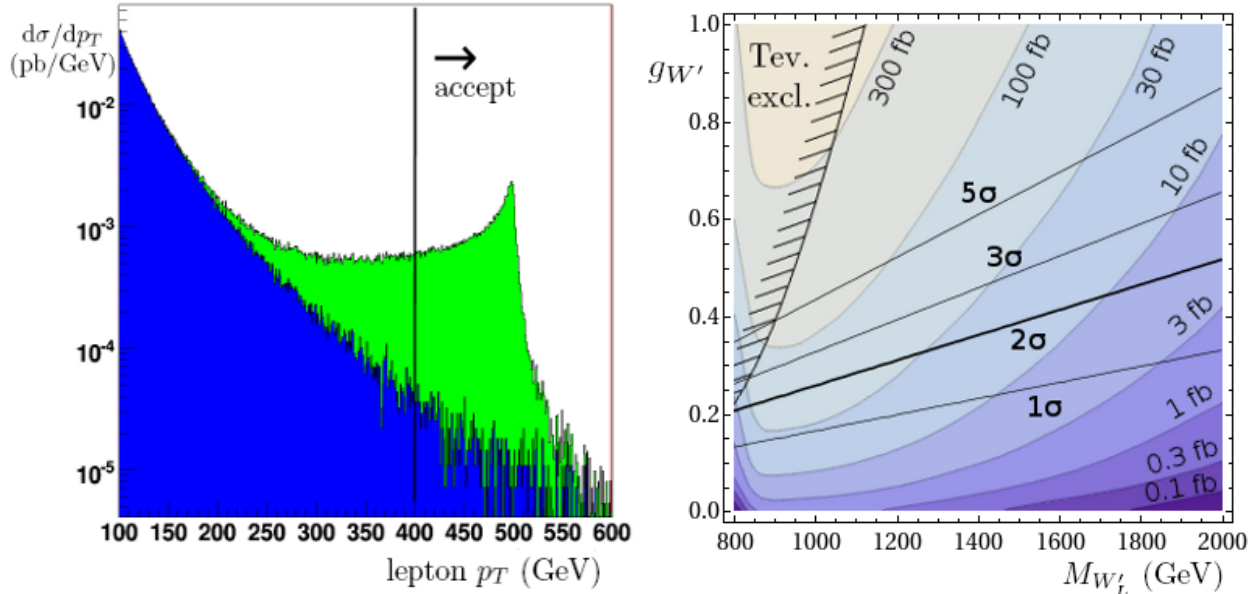


Figure 7: Left: Lepton p_T distribution for a W'_L signal with $M_{W'_L} = 1$ TeV and the irreducible Standard Model $W \rightarrow e\bar{\nu}_e$ background (blue). Right: Cross section \times branching ratio \times acceptance for the $W'_L \rightarrow e\nu_e$ signal at the 7 TeV LHC. Also shown are the limits from the Tevatron search and the electroweak precision fit.

5.1 $W'_L \rightarrow l\nu$ at the LHC

Let us discuss the decay of a W'_L to a lepton and a massless neutrino first. The expected signal of a hard lepton plus missing energy must be compared with the most relevant background from the high p_T tail of the W decay spectrum. We assume that all other Standard Model backgrounds such as $t\bar{t}$ and QCD dijet misidentification can be sufficiently reduced by appropriate cuts on the hadronic event activity, which is minimal in leptonic W'_L decays.²

Using MADGRAPH, we simulated the production and decay of W'_L bosons with masses between 800 GeV and 2 TeV and couplings up to $g_{W'} = 1$. At each model point, 1000 events were generated at the parton level. To estimate the background from the high p_T tail of $W \rightarrow l\nu$ events, we simulated 270k leptonic W decays with MADGRAPH, applying a lepton p_T cut of 100 GeV at the generator level. The cross section of this Standard Model background falls off steeply with p_T , such that only 2.8 background events with lepton $p_T > 400$ GeV are expected in each of the electron and muon channels for 1 fb^{-1} of LHC data. The results of our background simulation, compared with the expected signal for a 1 TeV W'_L boson with gauge coupling strength $g_{W'} \approx g'$, can be seen in the left half of Fig. 7.

We then simulated the production and decay of W'_L boson events with masses between 800 GeV and 2 TeV and couplings up to $g_{W'} = 1$ to find the effective cross section \times branching fraction \times signal efficiency. The resulting effective cross sections are shown as shaded contours in the right half of Fig. 7.

We also investigated the integrated luminosity required for discovery with 50 pb^{-1} and 1 fb^{-1} . For any integrated luminosity below 300 pb^{-1} , less than one background event is expected. We therefore assume that in this case 5 signal events after the lepton p_T cut are sufficient to establish the presence of new physics. With 1 fb^{-1} , the background is non-vanishing. We assume purely statistical errors and demand at least

²It should be noted that cosmic ray muons can falsely produce a $\mu + \text{MET}$ signal. However, we will not consider such events in our analysis, assuming that a good understanding of the detector and the use of timing information will reduce those backgrounds sufficiently.

$5\sqrt{N_{BG}} = 8.3$ signal events.

The W'_L has to be weakly coupled to avoid electroweak precision constraints. Our results suggest that such a sequential W'_L can not be found with the first 50 pb^{-1} of early LHC data. However, with 1 fb^{-1} of integrated luminosity, the LHC experiments become sensitive to a W'_L in the allowed region of parameter space with W'_L mass up to $\approx 1.5 \text{ TeV}$ and gauge coupling constant $g_{W'}$ smaller than g' . A W'_L with Standard Model like couplings is excluded by electroweak precision constraints up to several TeV (see the left panel of Figure 1.).

5.2 $W'_R \rightarrow lljj$ at the LHC

In the $W'_R \rightarrow lN$ two-body decay, the lepton is produced with fixed momentum

$$p_l = \frac{1}{2M_{W'_R}} \left(M_{W'_R}^2 - m_N^2 \right). \quad (34)$$

The lepton p_T distribution therefore exhibits a Jacobian peak at this value, corresponding to the events where the lepton is emitted perpendicularly to the beam pipe in the W'_R rest frame. For massless quarks and non-zero neutrino mass, the branching ratio for each leptonic decay mode is

$$BR(W'_R \rightarrow eN) = \frac{(1-x^2)^2(2+x^2)}{3(1-x^2)^2(2+x^2)+18}, \quad (35)$$

where $x = m_N/M_{W'_R}$ is the ratio of the neutrino and W'_R masses.

The heavy neutrino is unstable and decays via a virtual W'_R to another lepton and two jets. For large right-handed neutrino masses the resulting two leptons and two jets will be widely separated and easy to identify. Combining the jets with one of the leptons one obtains the invariant mass of the neutrino, combining both leptons and the jets one reconstructs $M_{W'_R}$.

For the right-handed W'_R decay to two hard leptons and two jets, we assume that all Standard Model backgrounds can be eliminated with appropriate cuts. This is certainly the case for same sign dilepton events, resulting from the decay of heavy Majorana neutrinos. For oppositely charged leptons plus jets, the most relevant backgrounds are Z/γ +jets, $t\bar{t}$ and pairs of electroweak gauge bosons. However, the the small integrated luminosity of less than 1 fb^{-1} at the early LHC implies that cuts on the dilepton mass and on the scalar transverse momentum sum result in an effectively background free sample. We therefore estimate the early LHC reach by demanding at least five signal events after basic kinematic cuts.

5.3 $W'_R \rightarrow lj_N$ at the LHC

If $M_{W'_R} \gg M_N$, the lepton and two jets from the heavy neutrino decay are emitted in a cone with opening angle

$$\Delta R \approx \frac{M_N}{M_{W'_R}}. \quad (36)$$

The event reconstruction at ATLAS and CMS by default implements the anti- k_T jet algorithm with cone sizes of $\Delta R_j = 0.4 - 0.7$. If the typical separation of the neutrino decay products is of this size or less, the two quarks can no longer be identified as separate objects but will instead appear as a single hadronic jet [24].

The “neutrino jet” is an object which will be interesting to search for at the LHC. It can be easily identified if it contains a hard muon, but even a boosted neutrino decaying into an electron and two hadronic subjets will produce a distinct signature that can be resolved using jet substructure techniques. Given the relative importance of this region in parameter space and the expected cleanliness of the final state signal (a hard lepton recoiling against a boosted neutrino jet) we believe that this case deserves a designated study. For

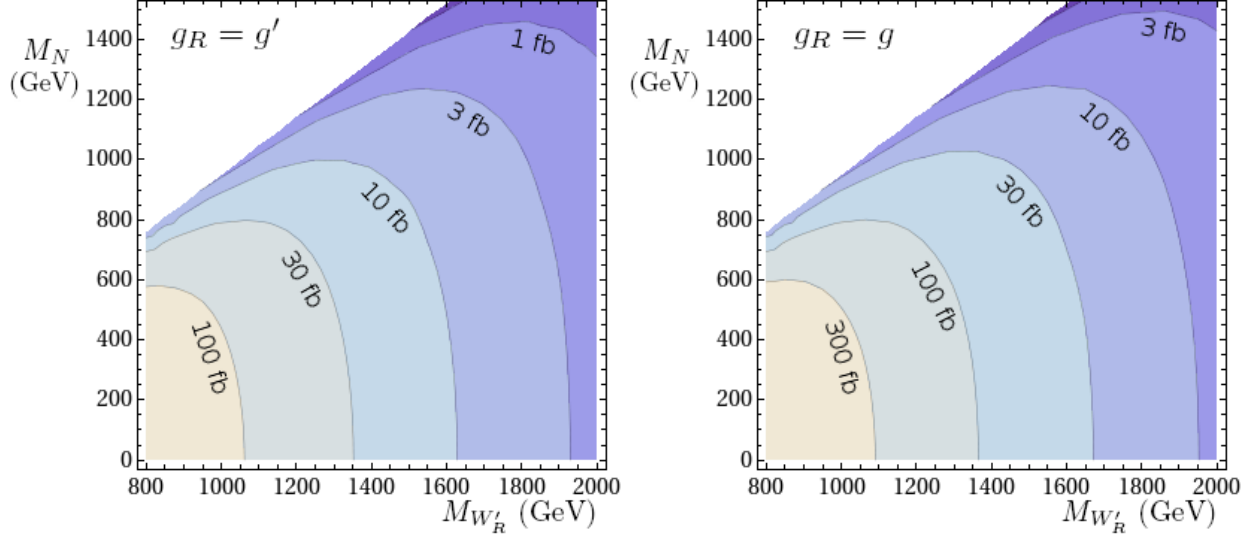


Figure 8: Effective cross section \times branching fraction for $W'_R \rightarrow eN$, as a function of the W'_R mass and the right-handed neutrino mass. Left: For coupling strength $g_{W'} = g'$, Right: for $g_{W'} = g$.

our plots we have assumed that the $\bar{l}j_N$ final state is easy to identify and has no Standard Model background, and our discovery contours correspond to 5 signal events.

How light can a right-handed neutrino be and have avoided detection so far? Since the right-handed neutrino is uncharged under the Standard Model gauge group, its only interaction with ordinary matter is through $W - W'_R$ and $Z - Z'$ mixing. The mixing angle α is of order $\mathcal{O}(v^2/f^2)$, so that the decays $Z \rightarrow NN$ and $W \rightarrow lN$ are suppressed by a factor of $\alpha^2 \approx 10^{-4}$ compared to the corresponding Standard Model decay modes into left-handed neutrinos. The only process in which right-handed neutrinos would have been produced in observable quantities is Z decay at LEP 1. The experimental bound on M_N is therefore the kinematic limit of $M_Z/2 \approx 45$ GeV.

5.4 $W'_R \rightarrow jj/tb$ at the LHC

It is also important to search for $W'_{L/R}$ bosons via decays to quarks which are necessarily present with large branching fractions if the W' can be produced at a Hadron collider. In the case of a decay to light quark jets, the QCD cross section for dijet production is orders of magnitude larger than a possible dijet W' signal. Furthermore, the shape and overall rate of the large invariant mass tail of the QCD background is not known accurately enough to establish the presence of a signal over the Standard Model background with the limited dataset available after the first two years of LHC running.

A search for W' decays into third generation quarks appears more promising, because the SM production of a top/bottom quark pair necessarily requires W exchange and is much smaller. The background to this signal is dominated by QCD events such as mistagged $q\bar{q}$ pair production with W-Strahlung or pair production of top quarks. A study of W' decays into boosted third generation quarks using jet substructure techniques would be interesting, but is beyond the scope of this paper.

6 Conclusions

W' searches are interesting examples of early physics for the LHC. The absence of strong indirect constraints from low energy measurements particularly motivates searches for the final states $l\bar{l}jj$ and $\bar{l}j_N$ from W'_R decays, already with 50 fb^{-1} of integrated luminosity. Note that in the case of a Majorana mass for the

right-handed neutrino the final state leptons can have the same or opposite sign charge with equal branching fractions.

We stress that searches for all possible W' final states

$$W'_L \rightarrow \begin{cases} l + \cancel{E}_T \\ t\bar{b} \\ jj \end{cases} \quad W'_R \rightarrow \begin{cases} \bar{l}ljj \\ l\bar{j}_N \\ t\bar{b} \\ jj \end{cases}$$

are interesting with larger data sets ($1\text{-}10 \text{ fb}^{-1}$). This is especially true if one keeps in mind that the final states which we have emphasized most may be closed due to phase space. In less universal models than the ones we have considered the W' may not couple to leptons at all so that only jj and $t\bar{b}$ final states are available. Finally, W' bosons may also decay to WZ and Wh with branching fractions which are suppressed by powers of v/f and are therefore less promising.

Acknowledgements

We wish to acknowledge useful conversations with Andy Cohen, Liam Fitzpatrick and Brock Tweedie and especially wish to thank Jesse Thaler for collaboration during the early stages of this project. This research is supported by the US Department of Energy under grant DE-FG02-01ER-40676.

A Splitting W'_R and Z'_R Bosons with Tensors

The Standard Model tree level relation

$$\frac{M_W}{M_Z} = \cos\theta_W, \quad (37)$$

i.e. $\rho = 1$, is a consequence of electroweak symmetry breaking with $SU(2)$ doublet Higgses. If the Higgses were taken to transform in higher $SU(2)$ representations, the relation would no longer be true and the Z would be relatively heavier. We can make use of this fact in the W'_R model to increase the mass splitting between Z'_R and W'_R . This is desirable because the precision electroweak constraints on W'_R models are dominated by Z'_R exchange.

To employ this in the context of the $SU(2)_R \times U(1)_X \rightarrow U(1)_Y$ model, at least two scalar fields are required. First, to raise the Z' mass we add a complex triplet field Δ with VEV

$$\langle \Delta \rangle = (0, 0, k/\sqrt{2}) \quad (38)$$

and a $U(1)$ charge of $+1$, so that hypercharge is unbroken. In order to write the Yukawa couplings for the Standard Model fermions we also need a doublet scalar H_R with a VEV $(0, f/\sqrt{2})$. The tree level masses of the gauge bosons are then

$$M_{Z'_R}^2 = \frac{1}{8} (g_R^2 + g_X^2) (4k^2 + f^2) \quad (39)$$

and

$$M_{W'_R}^2 = \frac{1}{8} g_R^2 (2k^2 + f^2). \quad (40)$$

In the limit $k \gg f$, the indirect EW precision constraint on the W'_R mass is therefore reduced by a factor $1/\sqrt{2}$. More generally, by using a scalar transforming in the D -dimensional representation of $SU(2)_R$ the indirect constraint on the W'_R is reduced by a factor of $1/\sqrt{D-1}$.

B Fermion Masses and $SU(2)_R$ Higgs Representations

In this Appendix we briefly discuss the issue of fermion masses and flavor. In models with full left-right symmetry at the TeV scale it is quite difficult to arrange for quark and lepton masses because the left-right symmetry predicts identical mass ratios for up- and down-type quarks as well as for charged and neutral leptons. Here, we have much more freedom because we are not interested to preserve even an approximate left-right symmetry at the TeV scale.

For example, we may obtain the Standard Model quark masses from the following operators

$$\mathcal{L}_Y = \lambda_u Q \phi Q^c + \frac{\lambda'}{\Lambda^2} (Q \phi H_R) (H_R^\dagger Q^c) \quad (41)$$

$$\rightarrow \lambda_u Q H_u u^c + \left(\lambda_u + \frac{\lambda' f^2}{2 \Lambda^2} \right) Q H_d d^c . \quad (42)$$

The use of the “projector” H_R onto the right-handed down quark allows for a splitting between up- and down-type masses without introducing tree level flavor changing neutral currents from Higgs exchange. As usual in theories with $SU(2)_R$ gauge bosons there are potentially disastrous box diagrams with W_L and W_R exchange which generate contributions to neutral meson mixing. The constraints from the neutral Kaon system for generic large right-handed flavor mixing angles are particularly severe and rule out W_R bosons near the TeV scale. These constraints are avoided if the right-handed CKM matrix takes on a specific form [38, 39]. We will ignore the constraint on the W_R mass and assume that excessive K-Kbar mixing is avoided by fortuitous right-handed mixing.

Even so, obtaining satisfactory lepton masses is a little tricky. The problem is that the operator

$$\lambda_e L \phi L^c \rightarrow \lambda_e L H_d e^c + \lambda_e L H_u \nu^c \quad (43)$$

adds unwanted large Dirac masses for neutrinos in addition to the charged lepton masses. Since the neutrino masses are 10 orders of magnitude smaller than the tau lepton mass, even a 4-loop radiatively generated coupling of the form Eq. (43) would give neutrino masses which are too large. Using the projector H_R does not help much in this case because the operator with $H_R H_R^\dagger$ radiatively generates the operator without H_R . Similarly, attempting to construct a model in which only one of the two Higgs doublets H_u and H_d obtains a VEV is problematic because radiative corrections generate a VEV for the other Higgs.

We circumvent this potential problem by including three generations of gauge singlet neutrinos N to marry off the unwanted right-handed neutrinos ν^c

$$\lambda_e L \tilde{\phi} L^c + \lambda_N N H_R L^c \rightarrow \lambda_e L H_u^* e^c + \lambda_e L H_d^* \nu^c + \frac{\lambda_N}{\sqrt{2}} f N \nu^c . \quad (44)$$

These couplings leave three generations of exactly massless neutrinos which are primarily the usual left-handed partners of the Standard Model charged leptons. The massless neutrinos contain a small admixture of N which alters their coupling to the W and Z . The mixing angle is suppressed by $\lambda_e v / (\lambda_N \tan \beta f)$ which is sufficiently small ($\sim 10^{-4}$) even for the neutrino partner of the tau lepton. Acceptable Standard Model neutrino masses can now be generated by adding a small violation of lepton number. For example, small majorana masses for N induce small majorana masses for the Standard Model neutrinos through mixing.

References

- [1] “LHC New Physics Working Group”, SLAC Theory Workshop, September 2010 [<http://lhcnwphysics.org/>]; J. Alwall, P. Schuster and N. Toro, “Simplified Models for a First Characterization of New Physics at the LHC,” Phys. Rev. D **79**, 075020 (2009) [arXiv:0810.3921 [hep-ph]].
- [2] R. N. Mohapatra and J. C. Pati, “A Natural Left-Right Symmetry,” Phys. Rev. D **11**, 2558 (1975).

- [3] R. N. Mohapatra and J. C. Pati, “Left-Right Gauge Symmetry And An Isoconjugate Model Of CP Violation,” *Phys. Rev. D* **11**, 566 (1975).
- [4] R. N. Mohapatra and G. Senjanovic, “Neutrino Masses And Mixings In Gauge Models With Spontaneous Parity Violation,” *Phys. Rev. D* **23**, 165 (1981).
- [5] R. S. Chivukula, B. Coleppa, S. Di Chiara, E. H. Simmons, H. J. He, M. Kurachi and M. Tanabashi, “A three site higgsless model,” *Phys. Rev. D* **74**, 075011 (2006) [arXiv:hep-ph/0607124].
- [6] V. D. Barger, W. Y. Keung and E. Ma, “A Gauge Model With Light W And Z Bosons,” *Phys. Rev. D* **22**, 727 (1980).
- [7] V. D. Barger, W. Y. Keung and E. Ma, “Doubling Of Weak Gauge Bosons In An Extension Of The Standard Model,” *Phys. Rev. Lett.* **44**, 1169 (1980).
- [8] H. Georgi, E. E. Jenkins and E. H. Simmons, “Ununifying The Standard Model,” *Phys. Rev. Lett.* **62**, 2789 (1989) [Erratum-ibid. **63**, 1540 (1989)].
- [9] H. Georgi, E. E. Jenkins and E. H. Simmons, “The Ununified Standard Model,” *Nucl. Phys. B* **331**, 541 (1990).
- [10] E. Malkawi, T. M. P. Tait and C.-P. Yuan, “A Model of strong flavor dynamics for the top quark,” *Phys. Lett. B* **385**, 304 (1996) [arXiv:hep-ph/9603349].
- [11] X. Li and E. Ma, “Gauge Model Of Generation Nonuniversality,” *Phys. Rev. Lett.* **47**, 1788 (1981).
- [12] X. G. He and G. Valencia, “The $Z \rightarrow b\bar{b}$ decay asymmetry and left-right models,” *Phys. Rev. D* **66**, 013004 (2002) [Erratum-ibid. **D 66**, 079901 (2002)] [arXiv:hep-ph/0203036].
- [13] N. Arkani-Hamed, A. G. Cohen and H. Georgi, “Electroweak symmetry breaking from dimensional deconstruction,” *Phys. Lett. B* **513**, 232 (2001); [arXiv:hep-ph/0105239]. N. Arkani-Hamed, A. G. Cohen, T. Gregoire and J. G. Wacker, “Phenomenology of electroweak symmetry breaking from theory space,” *JHEP* **0208**, 020 (2002). [arXiv:hep-ph/0202089].
- [14] N. Arkani-Hamed, A. G. Cohen, E. Katz and A. E. Nelson, “The lightest Higgs,” *JHEP* **0207**, 034 (2002). [arXiv:hep-ph/0206021].
- [15] M. Schmaltz and D. Tucker-Smith, “Little Higgs review,” *Ann. Rev. Nucl. Part. Sci.* **55**, 229 (2005); [arXiv:hep-ph/0502182]. M. Perelstein, “Little Higgs models and their phenomenology,” *Prog. Part. Nucl. Phys.* **58**, 247 (2007); [arXiv:hep-ph/0512128].
- [16] F. del Aguila, J. de Blas and M. Perez-Victoria, “Electroweak Limits on General New Vector Bosons,” *JHEP* **1009**, 033 (2010) [arXiv:1005.3998 [hep-ph]].
- [17] K. Hsieh, K. Schmitz, J. H. Yu and C. P. Yuan, “Global Analysis of General $SU(2) \times SU(2) \times U(1)$ Models with Precision Data,” *Phys. Rev. D* **82**, 035011 (2010) [arXiv:1003.3482 [hep-ph]].
- [18] T. G. Rizzo, “ Z' phenomenology and the LHC,” arXiv:hep-ph/0610104.
- [19] V. M. Abazov *et al.* [D0 Collaboration], “Search for W' bosons decaying to an electron and a neutrino with the D0 detector,” *Phys. Rev. Lett.* **100**, 031804 (2008) [arXiv:0710.2966 [hep-ex]].
- [20] T. Aaltonen *et al.* [The CDF Collaboration] “Search for new particles decaying to dijets in $p\bar{p}$ collisions at $\sqrt{s} = 1.96$ TeV,” CDF Note 9246 (2008)
- [21] V. M. Abazov *et al.* [D0 Collaboration], “Search for W' Boson Resonances Decaying to a Top Quark and a Bottom Quark,” *Phys. Rev. Lett.* **100**, 211803 (2008) [arXiv:0803.3256 [hep-ex]].

- [22] G. Aad *et al.* [The ATLAS Collaboration], “Expected Performance of the ATLAS Experiment - Detector, Trigger and Physics,” arXiv:0901.0512 [hep-ex].
- [23] G. L. Bayatian *et al.* [CMS Collaboration], “CMS technical design report, volume II: Physics performance,” *J. Phys. G* **34**, 995 (2007).
- [24] A. Ferrari *et al.*, “Sensitivity study for new gauge bosons and right-handed Majorana neutrinos in pp collisions at $s = 14$ -TeV,” *Phys. Rev. D* **62**, 013001 (2000).
- [25] S. N. Gninenko, M. M. Kirsanov, N. V. Krasnikov and V. A. Matveev, “Detection of heavy Majorana neutrinos and right-handed bosons,” *Phys. Atom. Nucl.* **70**, 441 (2007).
- [26] W. Y. Keung and G. Senjanovic, “Majorana Neutrinos And The Production Of The Right-Handed Charged Gauge Boson,” *Phys. Rev. Lett.* **50**, 1427 (1983).
- [27] S. Gopalakrishna, T. Han, I. Lewis, Z. g. Si and Y. F. Zhou, “Chiral Couplings of W' and Top Quark Polarization at the LHC,” arXiv:1008.3508 [hep-ph]; T. G. Rizzo, “The Determination of the Helicity of W' Boson Couplings at the LHC,” *JHEP* **0705**, 037 (2007) [arXiv:0704.0235 [hep-ph]]; M. Frank, A. Hayreter and I. Turan, “Production and Decays of W_R bosons at the LHC,” arXiv:1010.5809 [hep-ph].
- [28] C. W. Bauer, Z. Ligeti, M. Schmaltz *et al.*, “Supermodels for early LHC,” *Phys. Lett.* **B690**, 280-288 (2010). [arXiv:0909.5213 [hep-ph]].
- [29] K. Nakamura *et al.* [Particle Data Group], “Review of particle physics,” *J. Phys. G* **37**, 075021 (2010).
- [30] Z. Han and W. Skiba, “Effective theory analysis of precision electroweak data,” *Phys. Rev. D* **71**, 075009 (2005) [arXiv:hep-ph/0412166].
- [31] LEP Collaboration and ALEPH Collaboration and DELPHI Collaboration and L3 Collaboration and OPAL Collaboration and LEP Electroweak Working Group and SLD Electroweak Group and SLD Heavy Flavor Group, “A Combination of preliminary electroweak measurements and constraints on the standard model,” arXiv:hep-ex/0312023.
- [32] G. Cacciapaglia, C. Csaki, G. Marandella and A. Strumia, “The minimal set of electroweak precision parameters,” *Phys. Rev. D* **74**, 033011 (2006) [arXiv:hep-ph/0604111].
- [33] J. Alwall *et al.*, “MadGraph/MadEvent v4: The New Web Generation,” *JHEP* **0709**, 028 (2007) [arXiv:0706.2334 [hep-ph]].
- [34] V. M. Abazov *et al.* [D0 Collaboration], “Search for pair production of first-generation leptoquarks in $p\bar{p}$ collisions at $\sqrt{s}=1.96$ TeV,” *Phys. Lett. B* **681**, 224 (2009) [arXiv:0907.1048 [hep-ex]].
- [35] V. M. Abazov *et al.* [D0 Collaboration], “Search for pair production of second generation scalar leptoquarks,” *Phys. Lett. B* **671**, 224 (2009) [arXiv:0808.4023 [hep-ex]].
- [36] T. Sjostrand, S. Mrenna and P. Z. Skands, “PYTHIA 6.4 Physics and Manual,” *JHEP* **0605**, 026 (2006), [arXiv:hep-ph/0603175]. “A Brief Introduction to PYTHIA 8.1,” *Comput. Phys. Commun.* **178**, 852 (2008) [arXiv:0710.3820 [hep-ph]].
- [37] M. Drees and T. Han, “Signals for double parton scattering at the Fermilab Tevatron,” *Phys. Rev. Lett.* **77**, 4142 (1996) [arXiv:hep-ph/9605430].
- [38] P. Langacker and S. Uma Sankar, “Bounds on the Mass of $W(R)$ and the $W(L)$ - $W(R)$ Mixing Angle ξ in General $SU(2)$ - $L \times SU(2)$ - $R \times U(1)$ Models,” *Phys. Rev. D* **40**, 1569 (1989).
- [39] A. J. Buras, K. Gemmler and G. Isidori, “Quark flavour mixing with right-handed currents: an effective theory approach,” *Nucl. Phys. B* **843**, 107 (2011) [arXiv:1007.1993 [hep-ph]].